

## Research Article

# Adsorption Equilibrium for Heavy Metal Divalent Ions ( $\text{Cu}^{2+}$ , $\text{Zn}^{2+}$ , and $\text{Cd}^{2+}$ ) into Zirconium-Based Ferromagnetic Sorbent

**Agnes Yung Weng Lee, Soh Fong Lim, S. N. David Chua, Khairuddin Sanaullah, Rubiyah Baini, and Mohammad Omar Abdullah**

*Faculty of Engineering, Universiti Malaysia Sarawak, 94300 Kota Samarahan, Malaysia*

Correspondence should be addressed to Soh Fong Lim; [sflim@unimas.my](mailto:sflim@unimas.my)

Received 22 December 2016; Revised 19 March 2017; Accepted 6 April 2017; Published 5 July 2017

Academic Editor: Peter Majewski

Copyright © 2017 Agnes Yung Weng Lee et al. This is an open access article distributed under the Creative Commons Attribution License, which permits unrestricted use, distribution, and reproduction in any medium, provided the original work is properly cited.

Zirconium-based ferromagnetic sorbent was fabricated by coprecipitation of  $\text{Fe}^{2+}/\text{Fe}^{3+}$  salts in a zirconium solution and explored as a potential sorbent for removing the  $\text{Cu}^{2+}$ ,  $\text{Zn}^{2+}$ , and  $\text{Cd}^{2+}$  from aqueous solution. The sorbent could easily be separated from aqueous solution under the influence of external magnetic field due to the ferromagnetism property. A trimodal distribution was obtained for the sorbent with average particle size of  $22.74\ \mu\text{m}$ . The  $-\text{OH}$  functional groups played an important role for efficient removal of divalent ions. The surface of the sorbent was rough with abundant protuberance while the existence of divalent ions on the sorbent surface after the sorption process was demonstrated. Decontamination of the heavy metal ions was studied as a function of initial metal ions concentration and solution pH. Uptake of the heavy metal ions showed a pH-dependent profile with maximum sorption at around pH 5. The presence of the ferromagnetic sorbent in solution at different initial pH has shown a buffering effect. Equilibrium isotherms were analyzed using Langmuir, Freundlich, Dubinin-Radushkevich, and Temkin isotherm models. Adequacy of fit for the isotherm models based on evaluation of  $R^2$  and ARE has revealed that heavy metal ions decontamination was fitted well with the Freundlich model.

## 1. Introduction

Heavy metals are natural constituents of earth's crust, but indiscriminate human activities have drastically transformed their geochemical cycles and biochemical balance [1]. At present, pollution of aquatic ecosystems by the heavy metals is a significant problem as the heavy metals constitute certain most hazardous substances that can bioaccumulate in environment and ecosystem. Toxic metal compounds on the earth not only reach the earth's waters (seas, lakes, ponds, and reservoirs), but also can contaminate underground water in trace amounts by leaking from the soil after rain and snow [2]. The toxic metal ions dissolved can ultimately reach top of food chain and therefore developed a risk factor for human health besides causing ecological damage [3].

The risk of heavy metal pollution to public health and wildlife has led to an enlarged interest in development of effective technologies for water purification. Adsorption process has evolved into one of the prominent methods

for removing organic and inorganic pollutants in waterway systems [4]. This effective and economic process has been found superior to other techniques such as ion exchange and precipitation for treating aqueous effluents in terms of initial cost, simplicity of design, ease of operation, and insensitivity to toxic substances [5].

In recent years, the application of magnetic materials in solid phase extraction has received considerable attention by taking into account many advantages arising from the inherent characteristics of magnetic particles [6, 7]. The ferromagnetic sorbent can be easily recovered by magnetic separation technology and served as a satisfactory resolution for separation difficulty of ordinary powdered adsorbents. The ferromagnetic sorbent can simply be collected by an external magnetic field and such facile separation is essential to improving the operation efficiency. Additionally, the outstanding separation efficiency allows evacuation of the sorbent saturated with metal ions by means of magnetic captures, indicating a relatively simple technology without generation

of secondary effluents [8]. The magnetic separation technique combined with adsorption makes the wastewater treatment process simpler than applying a centrifugation or filtration.

Ferromagnetic iron oxide particles are the most favourable magnetic sorbents used in removal of pollutants due to their better magnetic properties, lower toxicity, and lower price [9, 10]. Besides, hexagonally ordered zirconia was shown to have high affinity towards  $\text{Co}^{2+}$ ,  $\text{Ni}^{2+}$ ,  $\text{Cu}^{2+}$ , and  $\text{Zn}^{2+}$  [11]. The findings herein are investigated for possibility of using the zirconium-based ferromagnetic sorbent for adsorptive removal of  $\text{Cu}^{2+}$ ,  $\text{Zn}^{2+}$ , and  $\text{Cd}^{2+}$  from aqueous solution. The dynamic behaviour of the metal ions sorption onto the ferromagnetic sorbent was studied with the effects of solution pH and initial metal ion concentration. The linear isotherm data analysis using two-parameter isotherm models was performed to validate the affinity between metal ions and aforementioned sorbent. In order to establish the most appropriate sorption equilibrium correlation, adequacy and accuracy in parameters prediction of the isotherm models were evaluated using error functions, regression coefficient ( $R^2$ ) and average relative error (ARE). The potential benefit of this study is to provide a certain theoretical basis for operational design and applicable practice of the sorption systems of heavy metals removal, which has drawn increasing attention in the area of water environmental protection.

## 2. Materials and Methods

**2.1. Materials.** All chemicals used were of analytical reagent grade and they were used without further purification. The raw materials for sorbent fabrication, zirconium(IV) sulfate ( $\text{Zr}(\text{SO}_4)_2$ ), iron(II) chloride ( $\text{FeCl}_2 \cdot 4\text{H}_2\text{O}$ ), and iron(III) chloride ( $\text{FeCl}_3 \cdot 6\text{H}_2\text{O}$ ), were obtained from Sigma-Aldrich Co. LLC whereas sodium hydroxide (NaOH) was obtained from Merck. The adsorbates, copper(II) sulfate ( $\text{CuSO}_4 \cdot 5\text{H}_2\text{O}$ ), zinc sulfate ( $\text{ZnSO}_4 \cdot 7\text{H}_2\text{O}$ ), and cadmium nitrate ( $\text{Cd}(\text{NO}_3)_2 \cdot 4\text{H}_2\text{O}$ ) were purchased from Fisher Scientific UK Ltd. The stock solution of  $\text{Cu}^{2+}$ ,  $\text{Zn}^{2+}$ , and  $\text{Cd}^{2+}$  was prepared by dissolving  $\text{CuSO}_4 \cdot 5\text{H}_2\text{O}$ ,  $\text{ZnSO}_4 \cdot 7\text{H}_2\text{O}$ , and  $\text{Cd}(\text{NO}_3)_2 \cdot 4\text{H}_2\text{O}$  in appropriate amounts of ultrapure water produced using Sartorius arium® pro ultrapure water system. All working solutions were freshly prepared by diluting the stock solutions to the desired concentrations, and initial pH value was adjusted to the designed values according to the following experimental design with hydrochloric acid (HCl) and sodium hydroxide (NaOH) solutions. The pH measurements were made using an Accumet AB15 pH meter equipped with a combine electrode (Fisher Scientific, USA).

**2.2. Fabrication of the Zirconium-Based Ferromagnetic Sorbent.** The zirconium-based ferromagnetic sorbent was fabricated according to the Lim [18] and Zheng et al. [19] chemical coprecipitation method with some modifications.  $\text{FeCl}_2 \cdot 4\text{H}_2\text{O}$  and  $\text{FeCl}_3 \cdot 6\text{H}_2\text{O}$  (1:2) were dissolved in ultrapure water. Zirconium sulfate solution was then injected into the mixed solution. The mixture was mechanically stirred with a Memmert water bath (Model WNE 14) and heated to

$70^\circ\text{C}$ . When the temperature was stabilized, 10 M of NaOH was added dropwise until the pH was above 8. Fe-Zr oxides were formed as the precipitate. The precipitate was washed until the pH of supernatant reached approximately 7. The precipitate was separated by magnetic decantation and dried in an oven (BINDER ED 53, Germany) at  $70^\circ\text{C}$  for 24 h. Finally, the obtained Fe-Zr sorbent was cooled at room temperature. The product was then ground in an agate mortar, appearing in the form of fine powders, subsequently sieved with a  $500\ \mu\text{m}$  stainless steel sieve, and kept at desiccator for further use.

**2.3. Instrumental Analyses of the Zirconium-Based Ferromagnetic Sorbent.** The particle size distribution of the zirconium-iron oxide particles was measured by Particle Size Analyzer (PSA) (CILAS 1090, French). The particle size analysis by laser diffraction gives measurement range from  $0.02\ \mu\text{m}$  to  $500\ \mu\text{m}$  in wet mode.

The surface functional groups of the zirconium-based ferromagnetic sorbent before and after metal ion adsorption were detected by an attenuated total reflectance (ATR) technique using a Fourier Transform Infrared (FT-IR) Spectroscopy (Shimadzu IRAffinity-1, Japan). Samples were measured by pressing them against a diamond prism that is positioned horizontally for the infrared microscope analysis. The infrared spectra were recorded in the IR wavelength between  $4000$  and  $400\ \text{cm}^{-1}$ . The spectra data was collected with twenty scans at a resolution of  $4\ \text{cm}^{-1}$  and the apodization function was of the Happ-Genzel type. All the spectra were recorded and plotted in the same scale on the transmittance axis.

Surface morphology of the ferromagnetic sorbent was studied by JEOL JSM-6390LA scanning electron microscope (SEM) with an embedded energy dispersive X-ray analyzer (EDS) for the elemental analysis of the ferromagnetic sorbent. The dry sample was mounted on aluminium plates using double-sided conductive carbon tape and sputter-coated with an Au film in vacuum using a JEOL JFC-1600 Auto Fine Coater prior to measurement. The coated sample was then visualized and examined with the scanning electron microscopy analysis operated at 10 kV. On the other hand, the qualitative EDS spectrum analyses on the specimen surface were conducted at 15 kV accelerating voltage and  $35^\circ$  take-off angle of X-ray at the analytical working distance of 10 mm. A probe current of 1 nA was raster-scanned across the specimens to minimize the risk of sample damage during imaging. All elements were readily observed and mapped using Smiling program.

Potentiometric titration was applied to study the acid-base properties of the ferromagnetic sorbent and the ionic exchange properties with regard to  $\text{H}^+$  and  $\text{OH}^-$  ions. The amount of 0.1 g of sorbent was added to 100 mL ultrapure water. A recorded volume of 0.1 M HCl was added to the mixture. The pH of each addition of acid was recorded in a time interval of 10 min. During the titration, the solution was gently shaken on the water bath and the experiment was carried out at  $25 \pm 1^\circ\text{C}$ . The experiment was repeated using 0.1 M NaOH to replace the 0.1 M HCl. The acid and base titration experiments were conducted separately.

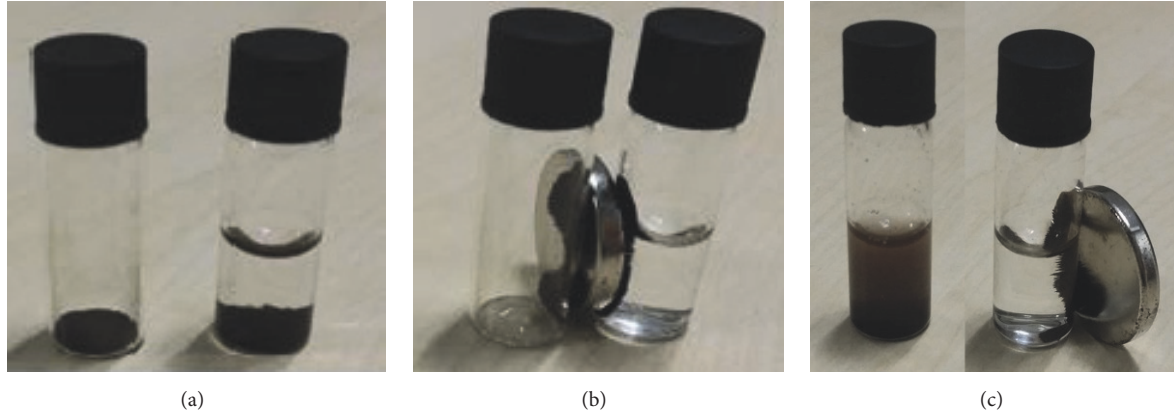


FIGURE 1: The zirconium-based ferromagnetic sorbent (a) under presence (wet) and absence (dry) of aqueous solution, (b) its magnetic responses under normal condition when being in contact with a permanent magnet, and (c) magnetic separation after sorption process.

### 3. Adsorption Experiments

**3.1. Equilibrium Study.** The heavy metal ions sorption isotherm was determined using batch experiments at varied initial metal ion concentration ranging from 5 to 350 mg/L. In each test, the sorbent at solid/solution ratio of 1 g/L was loaded in the 100 mL Erlenmeyer flasks with solution containing different concentration of heavy metal ion. The flasks were kept sealed in order to minimize losses to atmosphere. Next, the flasks were shaken in a refrigerated incubating shaker (Thermo Scientific 491, Japan) at 200 rpm for 24 h at  $25 \pm 1^\circ\text{C}$ . After the reaction period, all samples were filtered by  $0.45 \mu\text{m}$  membrane filter and analyzed for heavy metal ions using the atomic absorption spectrophotometer (AAS) (Shimadzu, AA-7000, Japan) equipped with  $\text{D}_2$  (deuterium lamp) method as a background correction, an air-acetylene burner, and controlled by the AA software, namely, WizAArd. The hollow cathode lamp was operated according to the elements of Cu, Zn, and Cd at 10 mA, 7 mA, and 5 mA whereas the analytical wavelength was set at 324.8 nm, 213.9 nm, and 228.8 nm, respectively. The amount of heavy metal ions adsorbed onto the sorbent ( $Q_e$ ) was calculated by mass balance equation of heavy metal ions before and after the sorption as expressed by

$$Q_e = \frac{(C_0 - C_e)V}{W}, \quad (1)$$

where  $C_0$  (mg/L) and  $C_e$  (mg/L) are the initial and equilibrated heavy metal ions concentrations, respectively,  $V$  (L) is the solution volume, and  $W$  (g) is the weight of the sorbent used. Correction for any sorption of heavy metal ions on the Erlenmeyer flask surface was made using the control experiment carried out under identical conditions in the absence of the zirconium-based ferromagnetic sorbent. These experiments indicated no detectable sorption by the Erlenmeyer flask surface and other factors.

**3.2. Effect of Solution pH Study.** Studies have been performed to identify the effect of solution pH on heavy metal ions sorption and uptake by the zirconium-based ferromagnetic

sorbent. The effect of solution pH was investigated in batch mode by varying the initial pH of the solution over the range of 2–7 with initial metal ion concentration, 50 mg/L, while keeping the other experimental conditions similar to equilibrium study. The experiments were carried out in triplicate in order to better understand the system.

**3.3. Estimation of Best Fitting Isotherm Models.** Over the past few decades, linear regression has been established as a major option in designing liquid-phase adsorption systems. Determination of the best isotherm model through analysis of regression coefficient ( $R^2$ ) is efficient but this indicator is limited to solving isotherm models that present linear forms [20]. Hence, average relative error (ARE) was employed in order to evaluate the fit of the isotherm equations to the experimental data and it is expressed as in

$$\text{ARE} = \frac{100}{n} \sum_{i=1}^n \left| \frac{q_{e,\text{exp}} - q_{e,\text{calc}}}{q_{e,\text{exp}}} \right|, \quad (2)$$

where  $q_{e,\text{exp}}$  and  $q_{e,\text{calc}}$  are the experimental and theoretically calculated adsorption capacity at equilibrium, respectively, while  $n$  is the number of data points.

### 4. Results and Discussion

**4.1. Characterization of the Zirconium-Based Ferromagnetic Sorbent.** The zirconium-based ferromagnetic sorbent is validated to have a good ferromagnetic property. As demonstrated in Figure 1, the ferromagnetic sorbent is attracted to a permanent magnet which is placed at outer wall of a glass vial that contains the sorbent. The magnetic attraction phenomenon occurs in both presence (wet) and absence (dry) of aqueous solution. Complementary to this, the magnetic sorbent also is able to be separated from dispersions with the application of a magnetic field after sorption process. Figure 1 illustrates that the sorbent is attracted and agglomerated with the aid of a permanent magnet and the supernatant is then discarded. The solution was observed to become limpid when the vial was placed near a permanent magnet

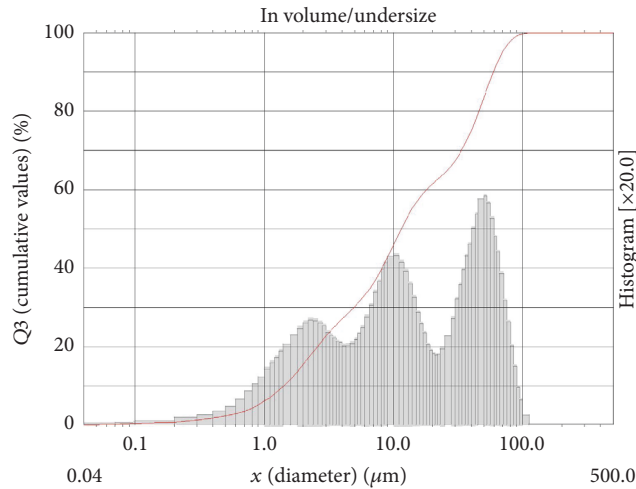


FIGURE 2: Particle size distribution of the zirconium-based ferromagnetic sorbent.

for a few seconds. This sorbent is used to adsorb heavy metal ions and subsequently isolated from the medium by the technique of magnetic separation. Once magnetized, the particles behave like small permanent magnets, thus forming lattice or aggregates due to magnetic interaction [7]. The zirconium-based ferromagnetic sorbent functionalized with the magnetic elements such as iron or oxides of iron and alloys enable the sorbent to have ferromagnetic properties that help rapid and easy separation of the new solid phase from the solution; thus avoiding the time consuming conventional column passing and filtration operations appeared to be promising especially in the case of environmental applications.

The particle size distribution is shown in Figure 2. It was found that this volume-based distribution of the ferromagnetic particles was in the range of  $0.06 \mu\text{m}$  to  $110 \mu\text{m}$  and the average particle size was  $22.74 \mu\text{m}$ . The analysis in the particles led to a trimodal distribution of the dispersion in the micron range. A larger fraction of the powdered particles was within the size range of  $20 \mu\text{m}$  to  $100 \mu\text{m}$  and the median particle size of the zirconium-iron oxide powders was  $11.52 \mu\text{m}$ .

Figure 3 displays the FT-IR spectra obtained for the ferromagnetic sorbent before and after sorption process. The analysis indicated that hydroxyl groups play an important role in the uptake. The stretching vibration of functional group  $-\text{OH}$  usually forms a broad band region within the range of  $3100\text{--}3700 \text{ cm}^{-1}$  for the presence of hydroxyl of coordinate water molecules. It was observed that those peaks have altered significantly after metal ion sorption, indicating the involvement in binding of the metal ion and ferromagnetic sorbent. Meanwhile, the prominent peaks at low frequency zone in the range of  $500\text{--}700 \text{ cm}^{-1}$  observed are due to metal oxygen stretching vibration which could be attributed to  $\text{ZrO}$  and  $\text{Fe-O}$  stretching vibration bond in the ferromagnetic sorbent. Besides, there were obvious additional peaks in the spectra after sorption (Samples (b)–(d)), showing evidences

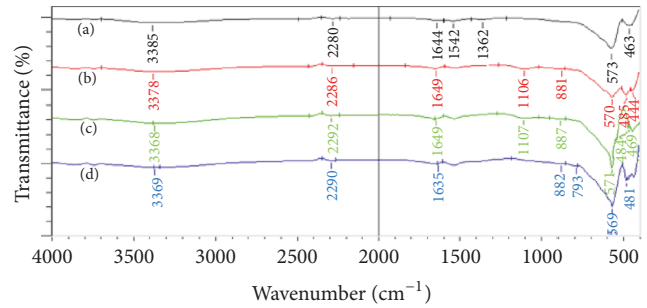


FIGURE 3: FT-IR spectra of the zirconium-based ferromagnetic sorbent (a) before and after sorption of (b)  $\text{Cu}^{2+}$ , (c)  $\text{Zn}^{2+}$ , and (d)  $\text{Cd}^{2+}$  [experimental conditions: sorbent dosage =  $1 \text{ g/L}$ , initial concentration =  $200 \text{ mg/L}$ , and contact time =  $24 \text{ h}$ ].

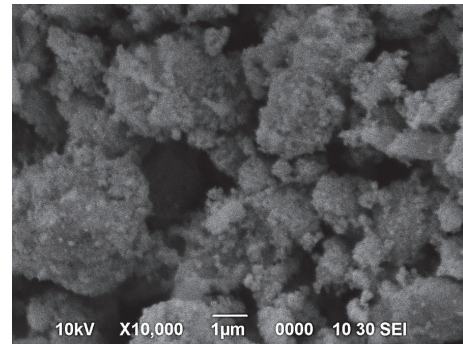


FIGURE 4: SEM micrograph of the zirconium-based ferromagnetic sorbent.

of  $\text{Fe-O-H}$  stretching ( $\sim 882 \text{ cm}^{-1}$ ) and bending ( $793 \text{ cm}^{-1}$ ) vibrations for adsorbed ion species. These imply that the  $-\text{OH}$  groups are involved during the metal ions sorption. Additionally, there is a peak on the multispectra around  $2300 \text{ cm}^{-1}$  that corresponds to the asymmetrical stretch of carbon dioxide ( $\text{CO}_2$ ), indicating  $\text{CO}_2$  in atmosphere is dissolved into the samples [21].

On the other hand, Figure 4 shows the SEM images of the ferromagnetic sorbent taken at a magnification capacity of  $\times 10000$  and a scale bar of  $1 \mu\text{m}$ . The sorbent particles with varying sizes agglomerated together appearing with irregular surface morphology. The surface of sorbent which was rough with abundant protuberance favoured the diffusion of metal ions into the ferromagnetic sorbent. The micrograph revealed irregularly shaped amorphous particles of the ferromagnetic sorbent similar to the characteristic of zirconia [22]. The existence of the very small sized particles along with the large agglomerates could be the explanation for the results obtained from particle size analysis where multimodal distribution was determined (Figure 2). The qualitative EDS spectrum analyses on the specimen surface were demonstrated in Figure 5. Based on Figure 5(a), the EDS spectrum revealed the energy spectrum of the X-ray character emitted from the element of iron (Fe), zirconium (Zr), and oxygen (O). Furthermore, no impurities were detected that would be attributable to contamination of chemical precursors. The

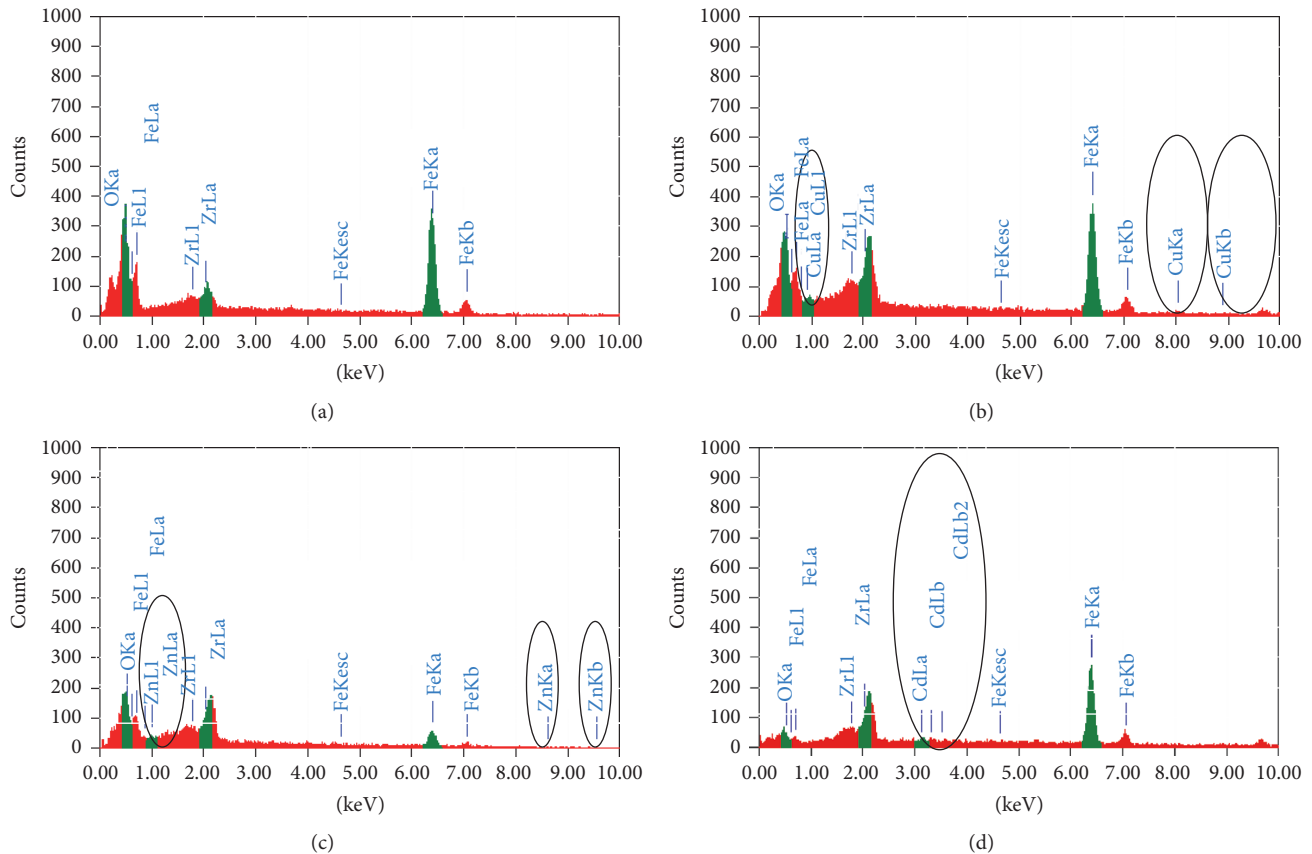


FIGURE 5: EDS spectra of the ferromagnetic sorbent (a) before and after adsorption of (b) Cu<sup>2+</sup>, (c) Zn<sup>2+</sup>, and (d) Cd<sup>2+</sup> [experimental conditions: sorbent dosage = 1 g/L, initial concentration = 200 mg/L, and contact time = 24 h].

existence of Cu<sup>2+</sup>, Zn<sup>2+</sup>, and Cd<sup>2+</sup> on the sorbent surface after the adsorption process could be observed accordingly comparing the EDS peaks with that of unloaded one, as presented in Figures 5(b)–5(d). It was suggested that the heavy metal ions have been adsorbed on the surface of the magnetic particles successfully.

Potentiometric titration was used to elucidate the functional groups on the ferromagnetic sorbent responsible for metal ions sorption. The acid-base nature of the zirconium-based magnetic sorbent and its equivalence point were identified. Based on Figure 6, the equivalence point of the titration curve was around pH 7 and the buffering zone was around pH 4 to pH 10. It was discovered that the ferromagnetic sorbent exhibited amphoteric behaviour where it could resist changes in pH upon the addition of small amount of acid or base. In order to further examine their behaviour, the effect of initial solution pH on the sorption process was performed and discussed in the section below.

**4.2. Effect of Initial Metal Ion Concentration.** The maximum sorption capacity obtained from the equilibrium studies was in the following order: Cu<sup>2+</sup> (48.4 mg/g) > Cd<sup>2+</sup> (30.9 mg/g) > Zn<sup>2+</sup> (29.2 mg/g) as presented in Figure 7, where the different sorption capacity may be due to disparity in cations radius

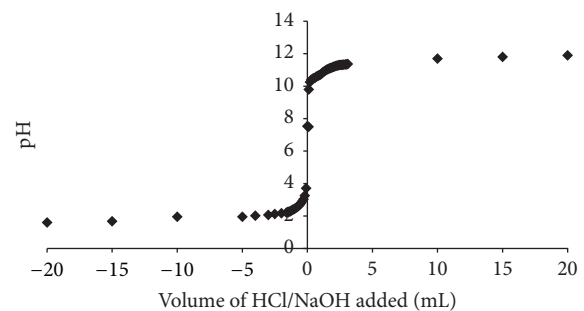


FIGURE 6: Titration curve of the zirconium-based ferromagnetic sorbent.

and interaction enthalpy values [23]. Comparison of maximum adsorption capacity of the zirconium-based ferromagnetic sorbent with various magnetic sorbents reported in literatures for Cu<sup>2+</sup>, Zn<sup>2+</sup>, and Cd<sup>2+</sup> adsorption is presented in Table 1. The adsorption capacity of the ferromagnetic sorbent was found to increase with the equilibrium concentrations of the metal ions in solution, progressively reaching saturation of the sorbent. The results indicated that when the metal ion concentration in the solution increased, the difference in concentration between bulk solution and surface also

TABLE 1: Comparison of maximum adsorption capacity of the zirconium-based ferromagnetic sorbent with various magnetic sorbents reported in literatures for  $\text{Cu}^{2+}$ ,  $\text{Zn}^{2+}$ , and  $\text{Cd}^{2+}$  adsorption.

Magnetic sorbents	Maximum adsorption capacity (mg/g)			Experimental conditions		References
	$\text{Cu}^{2+}$	$\text{Zn}^{2+}$	$\text{Cd}^{2+}$	Initial concentration (mg/L)	Adsorbent dosage (g/L)	
Zirconium-based magnetic sorbent	48.4	29.2	30.9	5–350	1	Present study
$\text{Fe}_3\text{O}_4$ /cyclodextrin polymer nanocomposites	—	—	27.7	50–400	12	Badruddoza et al. [12]
$\text{Fe}_3\text{O}_4$ magnetic nanoparticles (MNPs) modified with 3-aminopropyltriethoxysilane (APS) and copolymers of acrylic acid (AA) and crotonic acid (CA)	126.9	43.4	29.6	20–450	1	Ge et al. [13]
Magnetic ferric oxide doped vinyl benzene chloride divinylbenzene-based polymer	25.6	—	—	30	0.05–2	Simsek et al. [14]
Magnetic polymer beads with abundant amino groups	51.7	—	—	100–400	—	Lin et al. [15]
Magnetic $\text{Fe}_3\text{O}_4$ baker's yeast biomass	—	—	41.0	40–300	1	Xu et al. [16]
Iron oxide nanoparticles	—	—	18.5	10–600	10	Nassar [17]

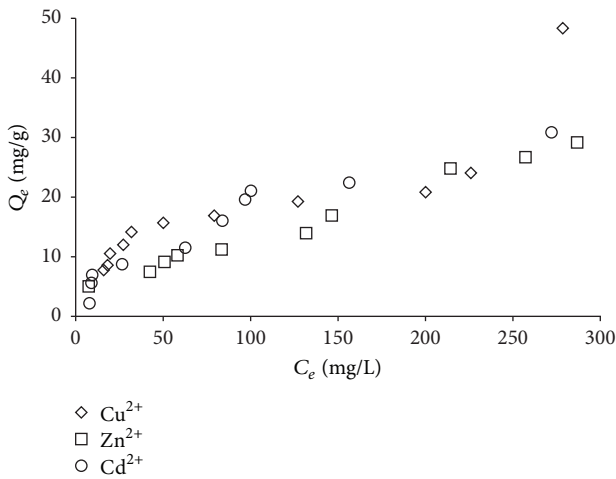


FIGURE 7: Adsorption capacity of the zirconium-based ferromagnetic sorbent for  $\text{Cu}^{2+}$ ,  $\text{Zn}^{2+}$ , and  $\text{Cd}^{2+}$  [experimental conditions: sorbent dosage = 1 g/L, contact time = 24 h, and temperature = 25°C].

increased hence intensifying the mass transfer processes [24]. This sorption characteristic suggested that surface saturation is dependent on the initial metal ion concentrations. At low concentrations, adsorption sites took up the available metal more rapidly, whereas at higher concentrations, metal ions need to diffuse to the sorbent surface by intraparticle diffusion and greatly hydrolyzed ions were diffused at a slower rate [25]. In the adsorption process, the metal ions were initially diffused from the boundary layer film onto the sorbent surface and finally diffuse into the porous structure of the sorbent.

**4.3. Effect of Initial Solution pH.** The solution pH of the sorbate solutions has been known as the most important parameter governing sorption of metal ions on different

sorbents. This may be due to the fact that hydrogen ions themselves are strong competing sorbate and the solution pH influences chemical speciation of metal ions [26]. The effect of surface characteristics of the sorption of metal ions from aqueous solution was correlated with the pH of the solution, as this affects the surface charge of the sorbents, solubility of metal ions, concentration of counterions on sorbent functional groups, and the degree of ionization of the sorbate [27].

The effect of initial solution pH on the heavy metal ions sorption by the zirconium-based ferromagnetic sorbent demonstrated in Figure 8(a) was strongly pH dependent. It was observed that the uptake of metal ions increased as the solution pH increased until the maximum uptakes were noted at pH around 5. As the pH of the solution increased to approximately 7, precipitation begins in the form of insoluble hydroxide,  $\text{M}(\text{OH})_2$ . Hence, it was believed that the sorption process became increasingly masked by precipitation and led to the increase of sorption capacity of  $\text{Zn}^{2+}$  and  $\text{Cd}^{2+}$  detected at pH around 7. Consequently, experiments were not conducted over pH 7 to avoid precipitation of metal complexes and hinder the distinction between adsorption and precipitation as heavy metals removal process [28]. The idea of working in a condition close to that naturally established by the medium without requiring significant modifications was also considered; the optimum pH for metal ions sorption was therefore determined to be 5 and applied in all experiments. Optimal sorption of inorganic divalent metal ions at this pH has been reported in numerous studies for rice bran, black gram husk, and Agbani clay [29–31].

The effect of solution pH on metal cation sorption is principally the result of changes in the net proton charge on particles. At low solution pH, the minimal sorption may be due to the higher concentration and high mobility of  $\text{H}^+$ , which are preferentially adsorbed rather than metal ions. The increase in positive charge density on the sorbent surface

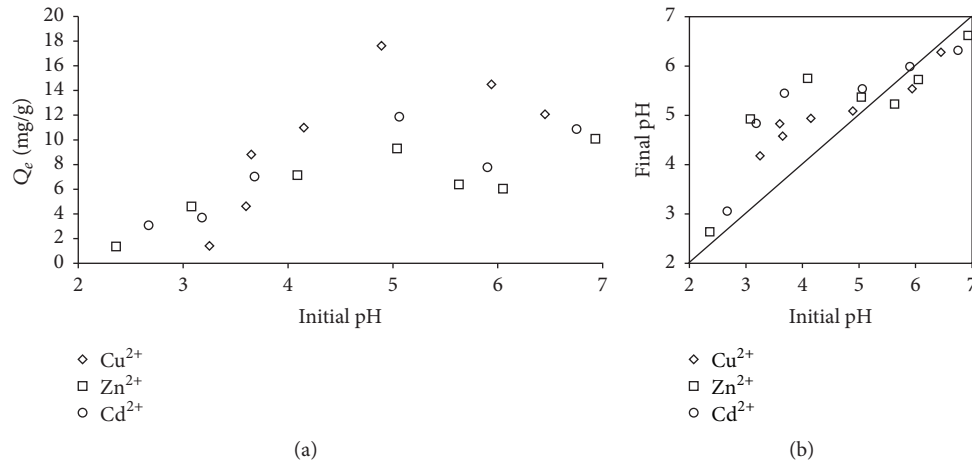
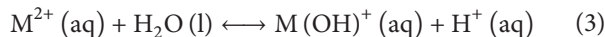


FIGURE 8: (a) Effect of initial solution pH and (b) initial solution pH versus final solution pH for the removal of  $\text{Cu}^{2+}$ ,  $\text{Zn}^{2+}$ , and  $\text{Cd}^{2+}$  by the zirconium-based ferromagnetic sorbent [experimental condition: initial concentration 50 mg/L].

sites resulted in electrostatic repulsion between the metal ion and positive charge on the sorption edges. In contrast, electrostatic repulsion decreases with increasing pH due to the increase in negative charge on the surface of sorbent thus enhancing metal cations sorption [32].

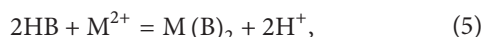
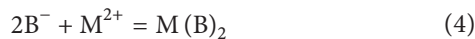
Similarly, the sorption would be retarded if the acidic environment was too strong to disturb the complex interaction of metal ions and functional group of the sorbent. This phenomenon has suggested that treatment with acid would enable regeneration of the ferromagnetic sorbent. Correspondingly, increasing of the solution pH value after saturation does not increase the metal ions sorption, but a partial metal ions desorption may occur due to the reaction of metal ions with  $\text{OH}^-$  ions and precipitate as a metal hydroxide [33].

The metal ions in the aqueous solution may undergo hydrolysis. Below pH 6, the dominant species of all metals are  $\text{M}^{2+}$  and  $\text{M}(\text{OH})^+$  [12]. Ghaffar [34] mentioned that simple hydrolysis of most divalent metal ions is written as



where  $\text{M}^{2+}$  represents  $\text{Cu}^{2+}$ ,  $\text{Zn}^{2+}$ , and  $\text{Cd}^{2+}$ . This reaction generates monovalent cations  $\text{M}(\text{OH})^+$  and protons which contribute to the increased acidity of  $\text{M}^{2+}$  solutions. If  $\text{M}^{2+}$  is being taken up by the sorbent, the reaction above shifts to the left, leading to the depletion of protons and accordingly a rise in pH value. The addition of NaOH to raise the pH before equilibration enhanced sorption of metal ions by the sorbent, suggesting that metal ion binding was occurring as carboxyl or hydroxyl ligands [35].

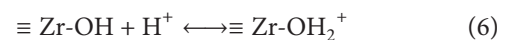
Additionally, Horsfall Jr. and Spiff [36] claimed that chemical bonding may be involved in metal adsorption; for instance, the  $\text{H}^+$  ions compete effectively with  $\text{M}^{2+}$  ions for sorption sites at low pH and the ion exchange mechanism may be represented in two ways as shown in



where  $\text{B}^-$  and B are polar sites on the sorbent surface.

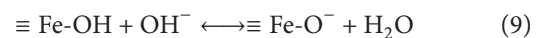
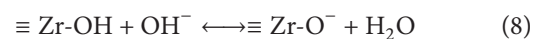
Furthermore, it was notable from Figure 8(b) that the reactions occurring during the sorption process caused slight fluctuation in the equilibrium pH. The equilibrium pH slightly increased as initial pH was below 5, whereas it decreased to lower values for initial pH above 5. These observations might be due to some buffering phenomena that occur during the sorption reaction. Good buffering capacity was shown at pH around 5 as mentioned in previous section which might be contributed by metal hydroxous oxides. It can be explained that zirconium and iron hydroxous oxides exhibit amphoteric surface hydroxyl sites in water [19]. Hydroxyl groups on metal oxide in water which can be protonated or deprotonated by the addition or deletion of hydrogen are the sites for ion exchange [37].

At a lower solution pH, the hydroxous oxides could be protonated as shown in



It is noteworthy that the sorbent surface binding sites are protonated; thereby  $\text{H}^+$  ions compete for active sorption sites on the surface of sorbent; this condition does not favour the uptake of cations leading to electrostatic repulsion. Due to the phenomena of competitive adsorption, the sorption of cations onto the surface of sorbent is decreased.

At a higher solution pH, the hydroxous oxides could be deprotonated as shown in



Nevertheless, an increase in pH produces a decrease in the positive surface charge as  $\text{OH}^-$  ions predominate. This condition leads to electrostatic force of attraction between the negatively charged surface of sorbent and cations as the sorbent becomes less repulsive to cationic species. This phenomenon favours the adsorption of cations, thus resulting in increased binding of positively charged metal ions.

In short, the adsorption mechanism is mainly contributed by the chemical interactions between the metal ions and the surface functional groups of the ferromagnetic sorbent. The increase in the adsorption of divalent ions with increasing pH indicates that an ion exchange mechanism between the  $H^+$  ions and metal ions occurs at the oxygen-containing functional groups on the sorbent surface. Based on the FT-IR analyses, the oxygen atoms of the hydroxyl groups donate their single pair of electrons to the metal ions, thus increasing the cation exchange capacity of the sorbent. Protons in the functional groups of the sorbent are exchanged with the metal ions. Chemical bonds between the metal ions and the surface functional groups of the zirconium-based ferromagnetic sorbent are mainly responsible for adsorption.

## 5. Adsorption Isotherms

The adsorption isotherms were mathematical models that described the distribution of the adsorbate species among the liquid and solid phases at the equilibrium state of an adsorption system. A state-of-the-art review of adsorption two-parameter isotherms models including Langmuir, Freundlich, Jovanovic, Dubinin-Radushkevich, Temkin, Flory-Huggins, and Hill isotherm models, their fundamental characteristics, and mathematical derivations was adopted to evaluate the decontamination of heavy metal ions by the zirconium-based ferromagnetic sorbent. The applicability of Langmuir, Freundlich, Dubinin-Radushkevich, and Temkin isotherm models is desirable to be presented for the isotherm analysis.

**5.1. Langmuir Isotherm Model.** The Langmuir isotherm model was derived based on the assumption of monolayer adsorption on a structurally homogeneous surface where there is no interaction between molecules adsorbed on neighbouring sites [38]. The linear form of the Langmuir isotherm is given by

$$\frac{C_e}{q_e} = \frac{1}{K_L q_m} + \frac{C_e}{q_m}, \quad (10)$$

where  $q_e$  (mg/g) is the sorbate amount sorbed on sorbent at equilibrium,  $K_L$  (L/mg) is Langmuir equilibrium constant, and  $q_m$  (mg/g) is the maximum monolayer coverage capacity. The Langmuir constants ( $K_L$  and  $q_m$ ) can be calculated from the plot of  $C_e/q_e$  versus  $C_e$ .  $K_L$  is related to the apparent energy of sorption and  $q_m$  reflects a complete monolayer (mg/g).

Moreover, the essential characteristics of Langmuir isotherm can be explained in terms of a dimensionless constant separation factor or equilibrium parameter  $R_L$ , which is defined by

$$R_L = \frac{1}{1 + K_L C_0}. \quad (11)$$

The value of  $R_L$  indicates the shape of the isotherm which is unfavourable ( $R_L > 1$ ), linear ( $R_L = 1$ ), favourable ( $0 < R_L < 1$ ), or irreversible ( $R_L = 0$ ).

TABLE 2: Isotherm parameters for sorption of heavy metal ions by the zirconium-based ferromagnetic sorbent.

Isotherm models	Cu <sup>2+</sup>	Zn <sup>2+</sup>	Cd <sup>2+</sup>
<i>Langmuir</i>			
$q_m$	38.1679	43.6681	39.0625
$K_L$	0.0133	0.0054	0.0104
<i>Freundlich</i>			
$1/n_F$	0.4441	0.5078	0.5845
$n_F$	2.2517	1.9693	1.7109
$K_F$	2.5704	1.3871	1.2306
<i>Dubinin-Radushkevich</i>			
$K_{DR}$	$5 \times 10^{-5}$	$1 \times 10^{-5}$	$2 \times 10^{-5}$
$E_{fe}$	0.10	0.22	0.16
$q_m$	22.4031	15.1500	18.4654
<i>Temkin</i>			
$b_T$	290.8	362.6	370.9
$A_T$	0.1398	0.1112	0.1922

Figure 9(a) depicts the plot of  $C_e/q_e$  versus  $C_e$  for the removal of heavy metal ions by using the zirconium-based ferromagnetic sorbent. From the plot, it was noticed that the sorption data were adequately fitted to the Langmuir equation with average regression coefficients ( $R^2 = 0.7130-0.8550$ ). The Langmuir constants obtained were computed in Table 2. The deviation of experimental data from the Langmuir isotherm may be due to the moderately homogeneous distribution of active sites on the surface of the ferromagnetic sorbent as this model introduced a clear concept of the monomolecular adsorption on energetically homogenous surfaces [39].

Additionally, the calculated equilibrium parameter,  $R_L$ , of the Langmuir isotherm was in the range between 0 and 1 for all the three heavy metal ions which indicate that the sorption processes were favourable.

**5.2. Freundlich Isotherm Model.** The Freundlich isotherm model is an empirical equation which represents the multi-layer adsorption on heterogeneous surfaces where there are interactions between adsorbed molecules [40]. Its linearized equation is illustrated as

$$\log(q_e) = \log(K_F) + \frac{1}{n_F} \log(C_e), \quad (12)$$

where  $K_F$  ( $mg^{1-(1/n)}L^{1/n}g^{-1}$ ) is the Freundlich constant and  $n_F$  is the constant of Freundlich equation exponent that represents the parameter characterizing quasi-Gaussian energetic heterogeneity of the adsorption surface. The  $K_F$  value is related to the adsorption capacity while the slope,  $1/n_F$ , ranging between 0 and 1 is a measure of adsorption intensity or surface heterogeneity, becoming more heterogeneous as its value gets closer to zero. However, a value below unity implies chemisorption process where  $1/n_F$  above one is indicative of cooperative adsorption [41, 42].



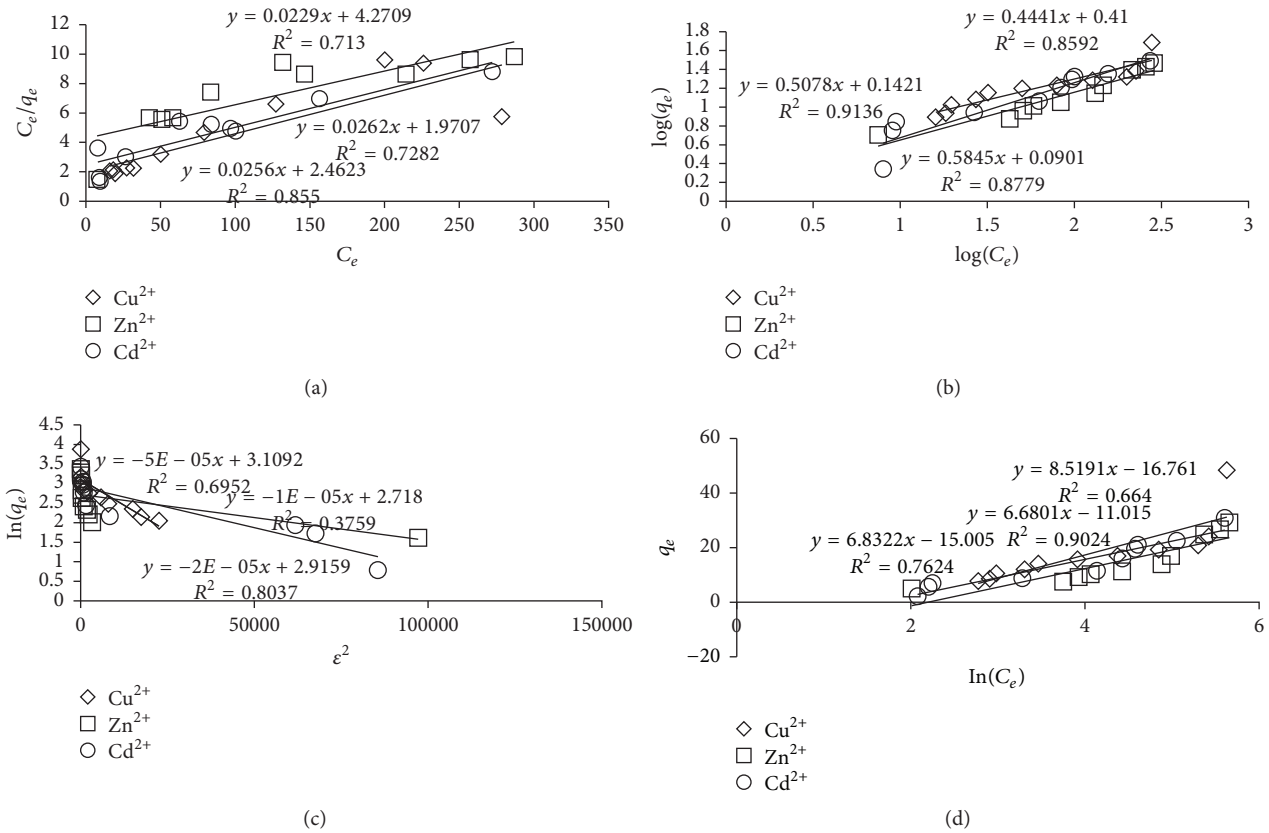


FIGURE 9: Plot for (a) Langmuir, (b) Freundlich, (c) Dubinin-Radushkevich, and (d) Temkin isotherm models for the removal of heavy metal ions by the zirconium-based ferromagnetic sorbent.

As presented in Figure 9(b), the Freundlich isotherm plot of  $\log(C_e)$  against  $\log(q_e)$  was fitted well with the experimental data. The  $n_F$  value indicates the degree of nonlinearity between solution concentration and adsorption where the values in the present study were found to be 1.7109–2.2517 (Table 2). This may be due to a distribution of surface sites or any factor that had caused a decrease in sorbent-sorbate interaction with increasing surface density. Besides, the  $n_F$  values lied within the range of 1–10 representing good adsorption [43].

Based on Table 2, the values of  $K_F$  obtained were 2.5704, 1.3871, and 1.2306 for Cu<sup>2+</sup>, Zn<sup>2+</sup>, and Cd<sup>2+</sup>, respectively. Increasingly large  $K_F$  value indicates greater adsorption capacity. It can be concluded here that the studied metal ions can be reduced using the ferromagnetic sorbent for high  $K_F$  value which has a large adsorption of capacity. This isotherm does not predict any saturation of the solid adsorbent surface; therefore infinite surface coverage is mathematically feasible. Furthermore, the linearity of the plot in Figure 9(b) has revealed the applicability of the Freundlich isotherm and shown that adsorption-complexation reactions may possibly take place in the adsorption process [44].

**5.3. Dubinin-Radushkevich Isotherm Model.** The Dubinin-Radushkevich isotherm model predicts the nature of the sorbate sorption onto the sorbent, and it is used to calculate the mean free energy of adsorption. This model is more general

than the Langmuir isotherm as its deviation is not based on ideal assumptions such as equipotential of sorption sites, absence of steric hindrances between sorbed and incoming particles, and surface homogeneity on microscopic level [45]. The isotherm has been written as

$$\ln(q_e) = \ln(q_m) - K_{DR}\epsilon^2, \quad (13)$$

where  $K_{DR}$  (mol<sup>2</sup>/J<sup>2</sup>) is D-R isotherm constant related to the adsorption energy and  $\epsilon$  is the Polanyi potential which is related to the equilibrium concentration and can be correlated as

$$\epsilon = RT \ln\left(1 + \frac{1}{C_e}\right), \quad (14)$$

where  $R$  is universal gas constant, 8.314 J/mol·K, and  $T$  is the absolute temperature at 298 K. The mean free energy of adsorption ( $E_{fe}$ ) per molecule of sorbate is calculated from the  $K_{DR}$  values using

$$E_{fe} = \frac{1}{\sqrt{2K_{DR}}}. \quad (15)$$

From the linear D-R isotherm plots for the sorption of the heavy metal ions onto the zirconium-based ferromagnetic sorbent,  $q_m$  was determined to be 22.4031 mg/g, 15.1500 mg/g, and 18.4654 mg/g for Cu<sup>2+</sup>, Zn<sup>2+</sup>, and Cd<sup>2+</sup>, respectively. The

TABLE 3: The comparison between correlation coefficient,  $R^2$ , and average relative error (ARE) among seven two-parameter isotherm models.

Isotherm models	$\text{Cu}^{2+}$		$\text{Zn}^{2+}$		$\text{Cd}^{2+}$	
	$R^2$	ARE (%)	$R^2$	ARE (%)	$R^2$	ARE (%)
Langmuir	0.7282	1.92	0.7130	4.96	0.8550	2.65
Freundlich	0.8592	3.20	0.9136	1.59	0.8779	0.56
Dubinin-Radushkevich	0.6952	4.90	0.3759	4.81	0.8037	4.03
Temkin	0.6640	3.23	0.7624	1.89	0.9024	1.44

value of  $q_m$  reveals the adsorption capacity performance; the higher the value of  $q_m$ , the better the adsorption capacity performance. Hence, the sorption process by the ferromagnetic sorbent shows the trend:  $\text{Cu} > \text{Cd} > \text{Zn}$ . The linear plots presented in Figure 9(c) and the analysis of the data showed that the experimental data do not correlate well with the D-R equation and this was confirmed by the regression coefficient shown in Table 3.

On the contrary, the mean free energy,  $E_{fc}$  was used to ascertain the type of adsorption process under consideration. The typical range of bonding energy for ion exchange mechanisms is 8–16 kJ/mol, indicating that chemisorption may play a significant role in the sorption process. In contrast, bonding energy values lower than 8 kJ/mol indicate that the sorption process is of a physical nature. In this study, the calculated  $E_{fc}$  values were limited within the range of 0.10–0.22 kJ/mol, indicating that the removal of heavy metal ions by using the ferromagnetic sorbent occurs via physisorption. According to A. U. Itodo and H. U. Itodo [45], physisorption is also called nonspecific adsorption which occurs as a result of long range weak Van der Waals forces between adsorbates and sorbents whereas the energy released when a particle is physisorbed is of the same magnitude as the enthalpy of condensation. In physical adsorption, equilibrium is established between the adsorbate and the fluid phase resulting in multilayer adsorption. Then, again, both physisorption and chemisorption may occur on the surface at the same time in some cases where a layer of molecules may be physically adsorbed on top of an underlying chemisorbed layer [46].

**5.4. Temkin Isotherm Model.** Temkin isotherm encloses a factor explicitly taking into account sorbent-sorbate interactions [47]. The model assumes that the adsorption heat of all molecules decreases linearly with the increase in coverage of the adsorbent surface. As implied in the equation, its derivation is characterized by a uniform distribution of binding energies (up to some maximum binding energy). A linear form of the Temkin equation can be expressed as

$$q_e = \frac{RT}{b_T} \ln(A_T) + \frac{RT}{b_T} \ln(C_e), \quad (16)$$

where  $A_T$  (L/g) is equilibrium binding constant corresponding to the maximum binding energy and  $b_T$  (J/mol) is the variation of adsorption energy. By plotting the quantity sorbed,  $q_e$  versus  $\ln C_e$ , the constants can hence be determined from the slope and intercept.

By referring to Figure 9(d), the equilibrium binding constant,  $A_T$ , was found to be 0.1398 L/g, 0.1112 L/g, and

0.1922 L/g while the variation of adsorption energy,  $b_T$ , is 290.8 J/mol, 362.6 J/mol, and 370.9 J/mol for  $\text{Cu}^{2+}$ ,  $\text{Zn}^{2+}$ , and  $\text{Cd}^{2+}$ , respectively. The corresponding parameters and the regression coefficients of Temkin model were presented in Tables 2 and 3.

Apart from that, the low values of typical range of bonding energy,  $RT/b_T$ , in this study indicated a weak interaction between sorbent and sorbate supporting a mechanism of ion exchange and the adsorption energy of all the molecules in the surface layer decreased at the cover surface. Higher values of the coefficient of correlation show a good linearity regardless of the maximum capacity of adsorption used to calculate the coverage area. Consequently, the Temkin isotherm can describe reasonably well the sorption isotherms of heavy metal ions onto the ferromagnetic sorbent with  $R^2 = 0.6640$ – $0.9024$ .

**5.5. Comparison between Isotherm Models.** The typical assessment of the quality of the isotherm fit to the experimental data was based on the magnitude of the correlation coefficient for the regression. The values of regression coefficient,  $R^2$ , from the linearization of the four two-parameter isotherm models and the corresponding average relative error (ARE) obtained were listed in Table 3. The ARE based on (2) gives small values when the data obtained from the model are comparable to the experimental data. It was noticed that the aforementioned isotherm models were appropriate in their own merits in describing the potential of the zirconium-based ferromagnetic sorbent for the removal of  $\text{Cu}^{2+}$ ,  $\text{Zn}^{2+}$ , and  $\text{Cd}^{2+}$  from aqueous solution.

Consideration of the comparative magnitudes of the  $R^2$  and ARE had suggested that the Freundlich isotherm model provided a better model for the sorption systems. A plausible reason of this observation is that this isotherm requires the taking of logarithms, therefore introducing similar effects to the error structure. As the Freundlich equation describes adsorption where the adsorbent has a heterogeneous surface with adsorption sites that have different energies of adsorption, the presence of zirconium dioxide in the ferromagnetic sorbent may lead to a more heterogeneous surface [48].

The results were comparable to the previous works related to the removal of metal heavy ions onto various magnetic sorbents done by other researchers. For instance, Ehrampoush et al. [49] have observed that the adsorption of cadmium ions from aqueous solution by synthesized iron oxide nanoparticles with tangerine peel extract followed Freundlich model better than Langmuir model according to

the regression coefficient. Charpentier et al. [50] also claimed that Freundlich model was found to be more accurate when describing the adsorption of  $\text{Cu}^{2+}$  and  $\text{Zn}^{2+}$  on magnetic carboxymethyl chitosan nanocomposites as the mechanism is in agreement with the good fitting of the experimental data with the Freundlich adsorption isotherm. Moreover, the isotherm data of removal of  $\text{Cd}^{2+}$  from aqueous solution by shellac-coated iron oxide nanoparticles as an effective magnetic nanoparticle adsorbent were validated to be well fit with Freundlich isotherm with the maximum adsorption capacity, 18.8 mg/g at pH = 8 [51].

## 6. Conclusions

The present investigation demonstrated that the zirconium-based ferromagnetic sorbent fabricated by chemical coprecipitation method exhibited good performance to remove heavy metal ions ( $\text{Cu}^{2+}$ ,  $\text{Zn}^{2+}$ , and  $\text{Cd}^{2+}$ ) from aqueous solution. Instrumental analyses were performed using Particle Size Analyzer (PSA), Fourier Transform Infrared (FT-IR) Spectroscopy, and scanning electron microscopic-energy dispersive X-ray spectroscopy (SEM-EDS). The batch studies revealed that the sorption process was highly solution pH dependent. The sorption capacity was reduced when the solution was in strong acidic condition and reached the maximum at pH around 5. Equilibrium adsorption isotherms were measured for single component system and the experimental data were analyzed with four two-parameter isotherm models, namely, the Langmuir, Freundlich, Dubinin-Radushkevich, and Temkin isotherm equations. Two mathematically rigorous error functions, regression coefficient ( $R^2$ ) and average relative error (ARE), have been addressed to evaluate the fitting ability of these models. Examination of the linear isotherm plots suggested that the Freundlich model yielded a better fit than all other models, indicating a heterogeneous surface of the zirconium-based ferromagnetic sorbent and multilayer adsorption nature of the decontamination process. Apart from that, the Freundlich constant ( $n_F$ ), which was estimated to be greater than 1 proved that the sorption of heavy metal ions from the aqueous solution was favourable. Due to the undeniable advantages of the zirconium-based ferromagnetic sorbent such as inexpensive preparation method and easy separation on application of magnetic field, it was noteworthy that the sorbent can be a potential candidate for the decontamination of heavy metal ions from industrial effluents.

## Conflicts of Interest

The authors declare that there are no conflicts of interest regarding the publication of this paper.

## Acknowledgments

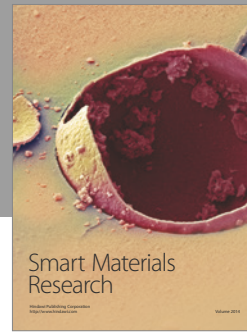
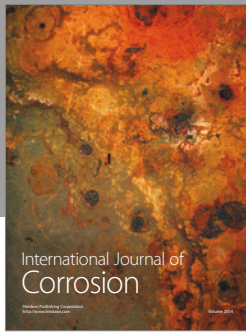
This research was funded by Special Grant Scheme (F02/SpGS/1404/16/5) from Universiti Malaysia Sarawak.

## References

- [1] R. Singh, N. Gautam, A. Mishra, and R. Gupta, "Heavy metals and living systems: an overview," *Indian Journal of Pharmacology*, vol. 43, no. 3, pp. 246–253, 2011.
- [2] I. Uzun and F. Güzel, "Adsorption of some heavy metal ions from aqueous solution by activated carbon and comparison of percent adsorption results of activated carbon with those of some other adsorbents," *Turkish Journal of Chemistry*, vol. 24, no. 3, pp. 291–297, 2000.
- [3] T. G. Merlain, N. J. Nsami, and K. J. Mbadcam, "Adsorption of copper (II) ions from aqueous solution onto synthetic goethite and two naturally available red soils from Yaoundé-Cameroon," *British Biotechnology Journal*, vol. 3, no. 3, pp. 221–235, 2013.
- [4] N. Barka, S. Qourzal, A. Assabbane, A. Nounah, and Y. Ait-Ichou, "Removal of Reactive Yellow 84 from aqueous solutions by adsorption onto hydroxyapatite," *Journal of Saudi Chemical Society*, vol. 15, no. 3, pp. 263–267, 2011.
- [5] K. T. Dauda, V. N. Atasi, and O. B. Adeoye, "The kinetics and equilibrium studies of the adsorption of ( $\text{Cu}^{2+}$ ,  $\text{Pb}^{2+}$ ) from industrial wastewater using rice husk as adsorbent," *International Journal of Advanced Research in Chemical Science*, vol. 2, no. 4, pp. 13–21, 2015.
- [6] S.-F. Lim, Y.-M. Zheng, S.-W. Zou, and J. P. Chen, "Characterization of copper adsorption onto an alginate encapsulated magnetic sorbent by a combined FT-IR, XPS, and mathematical modeling study," *Environmental Science and Technology*, vol. 42, no. 7, pp. 2551–2556, 2008.
- [7] G. Giakissikli and A. N. Anthemidis, "Magnetic materials as sorbents for metal/metalloid preconcentration and/or separation. A review," *Analytica Chimica Acta*, vol. 789, pp. 1–16, 2013.
- [8] M. Yamaura and D. A. Fungaro, "Synthesis and characterization of magnetic adsorbent prepared by magnetite nanoparticles and zeolite from coal fly ash," *Journal of Materials Science*, vol. 48, no. 14, pp. 5093–5101, 2013.
- [9] S.-F. Lim, Y.-M. Zheng, S.-W. Zou, and J. P. Chen, "Removal of copper by calcium alginate encapsulated magnetic sorbent," *Chemical Engineering Journal*, vol. 152, no. 2-3, pp. 509–513, 2009.
- [10] N. Rahbar, Z. Ramezani, and Z. Mashhadizadeh, "One step in-situ formed magnetic chitosan nanoparticles as an efficient sorbent for removal of mercury ions from petrochemical waste water: batch and column study," *Jundishapur Journal of Health Sciences*, vol. 7, no. 4, pp. 13–19, 2015.
- [11] R. F. De Farias, A. A. S. Do Nascimento, and C. W. B. Bezerra, "Adsorption of Co(II), Ni(II), Cu(II), and Zn(II) on hexagonal templated zirconia obtained thorough a sol-gel process: the effects of nanostructure on adsorption features," *Journal of Colloid and Interface Science*, vol. 277, no. 1, pp. 19–22, 2004.
- [12] A. Z. M. Badruddoza, Z. B. Z. Shawon, W. J. D. Tay, K. Hidajat, and M. S. Uddin, " $\text{Fe}_3\text{O}_4$ /cyclodextrin polymer nanocomposites for selective heavy metals removal from industrial wastewater," *Carbohydrate Polymers*, vol. 91, no. 1, pp. 322–332, 2013.
- [13] F. Ge, M. M. Li, H. Ye, and B. X. Zhao, "Effective removal of heavy metal ions  $\text{Cd}^{2+}$ ,  $\text{Zn}^{2+}$ ,  $\text{Pb}^{2+}$ ,  $\text{Cu}^{2+}$  from aqueous solution by polymer-modified magnetic nanoparticles," *Journal of Hazardous Materials*, vol. 211, pp. 366–372, 2012.
- [14] E. B. Simsek, D. Duranoglu, and U. Beker, "Heavy metal adsorption by magnetic hybrid-sorbent: an experimental and theoretical approach," *Separation Science and Technology*, vol. 47, no. 9, pp. 1334–1340, 2012.

- [15] Z. Lin, Y. Zhang, Y. Chen, and H. Qian, "Extraction and recycling utilization of metal ions ( $\text{Cu}^{2+}$ ,  $\text{Co}^{2+}$  and  $\text{Ni}^{2+}$ ) with magnetic polymer beads," *Chemical Engineering Journal*, vol. 200, pp. 104–112, 2012.
- [16] M. Xu, Y. Zhang, Z. Zhang, Y. Shen, M. Zhao, and G. Pan, "Study on the adsorption of  $\text{Ca}^{2+}$ ,  $\text{Cd}^{2+}$  and  $\text{Pb}^{2+}$  by magnetic  $\text{Fe}_3\text{O}_4$  yeast treated with EDTA dianhydride," *Chemical Engineering Journal*, vol. 168, no. 2, pp. 737–745, 2011.
- [17] N. N. Nassar, "Kinetics, equilibrium and thermodynamic studies on the adsorptive removal of nickel, cadmium and cobalt from wastewater by superparamagnetic iron oxide nanoadsorbents," *Canadian Journal of Chemical Engineering*, vol. 90, no. 5, pp. 1231–1238, 2012.
- [18] S. F. Lim, *Adsorption of contaminations by magnetic sorbents [Ph.D. thesis]*, National University of Singapore, 2008, Retrieved from National University of Singapore Digital Theses.
- [19] Y. M. Zheng, S. F. Lim, and J. P. Chen, "Preparation and characterization of zirconium-based magnetic sorbent for arsenate removal," *Journal of Colloid and Interface Science*, vol. 338, no. 1, pp. 22–29, 2009.
- [20] J. S. Piccin, G. L. Dotto, and L. A. A. Pinto, "Adsorption isotherms and thermochemical data of FDandC RED No 40 Binding by chitosan," *Brazilian Journal of Chemical Engineering*, vol. 28, no. 2, pp. 295–304, 2011.
- [21] S.-F. Lim and A. Y. W. Lee, "Kinetic study on removal of heavy metal ions from aqueous solution by using soil," *Environmental Science and Pollution Research*, vol. 22, no. 13, pp. 10144–10158, 2015.
- [22] F. J. Pereira, M. T. Díez, and A. J. Aller, "Effect of temperature on the crystallinity, size and fluorescent properties of zirconia-based nanoparticles," *Materials Chemistry and Physics*, vol. 152, pp. 135–146, 2015.
- [23] T. Madrakian, A. Afkhami, B. Zadpour, and M. Ahmadi, "New synthetic mercaptoethylamino homopolymer-modified maghemite nanoparticles for effective removal of some heavy metal ions from aqueous solution," *Journal of Industrial and Engineering Chemistry*, vol. 21, pp. 1160–1166, 2015.
- [24] B. Nagy, B. Szilagyí, C. Majdik, G. Katona, C. Indolean, and A. Máicáneau, "Cd (II) and Zn (II) biosorption on *Lactarius piperatus* macrofungus: equilibrium isotherm and kinetic studies," *Environmental Progress and Sustainable Energy*, vol. 33, no. 4, pp. 1158–1170, 2014.
- [25] S. E. Oh, S. H. A. Hassan, and J. H. Joo, "Biosorption of heavy metals by phylized cells of *Pseudomonas stutzeri*," *World Journal of Microbiology and Biotechnology*, vol. 25, no. 10, pp. 1771–1778, 2009.
- [26] A. Rajappa, K. Ramesh, and V. Nandhakumar, "Adsorption of nickel(II) ion from aqueous solution onto  $\text{ZnCl}_2$  activated carbon prepared from *Delonix regia* pods (flame tree)," *International Journal of Chemical and Physical Sciences*, vol. 3, no. 6, pp. 42–52, 2014.
- [27] N. Rajamohan, M. Rajasimman, R. Rajeshkannan, and V. Saravanan, "Equilibrium, kinetic and thermodynamic studies on the removal of Aluminum by modified *Eucalyptus camaldulensis* barks," *Alexandria Engineering Journal*, vol. 53, no. 2, pp. 409–415, 2014.
- [28] M. M. A. El-Latif, A. M. Ibrahim, M. S. Showman, and R. R. A. Hamide, "Alumina/Iron oxide nano composite for cadmium ions removal from aqueous solutions," *International Journal of Nonferrous Metallurgy*, vol. 2, pp. 47–62, 2013.
- [29] S. F. Montanher, E. A. Oliveira, and M. C. Rollemberg, "Removal of metal ions from aqueous solutions by sorption onto rice bran," *Journal of Hazardous Materials*, vol. 117, no. 2-3, pp. 207–211, 2005.
- [30] A. Saeed, M. Iqbal, and M. W. Akhtar, "Removal and recovery of lead(II) from single and multimetal (Cd, Cu, Ni, Zn) solutions by crop milling waste (black gram husk)," *Journal of Hazardous Materials*, vol. 117, no. 1, pp. 65–73, 2005.
- [31] F. A. Dawodu, G. K. Akpomie, and I. C. Ogbu, "Isotherm modelling on the equilibrium sorption of cadmium (II) from solution by Agbani clay," *International Journal of Multidisciplinary Sciences and Engineering*, vol. 3, no. 9, pp. 9–14, 2012.
- [32] Th. Bohli, A. Ouederni, N. Fiol, and I. Villaescusa, "Uptake of  $\text{Cd}^{2+}$  and  $\text{Ni}^{2+}$  metal ions from aqueous solutions by activated carbons derived from waste olive stones," *International Journal of Chemical Engineering and Applications*, vol. 3, no. 4, pp. 232–236, 2012.
- [33] M. E. Goher, A. M. Hassan, I. A. Abdel-Moniem, A. H. Fahmy, M. H. Abdo, and S. M. El-sayed, "Removal of aluminum, iron and manganese ions from industrial wastes using granular activated carbon and Amberlite IR-120H," *Egyptian Journal of Aquatic Research*, vol. 41, no. 2, pp. 155–164, 2015.
- [34] A. Ghaffar, "Removal of lead(II) ions from aqueous solution under different physicochemical conditions using various sorbents," *Arabian Journal for Science and Engineering*, vol. 33, no. 1A, pp. 55–61, 2008.
- [35] C. I. Osu and S. A. Odoemelan, "Studies on adsorbent dosage, particle sizes and pH constraints on biosorption of Pb(II) and Cd(II) ions from aqueous solution using modified and unmodified *Crasotrea Gasar* (bivalve) biomass," *Report and Opinion*, vol. 6, no. 12, pp. 67–72, 2014.
- [36] M. Horsfall Jr. and A. I. Spiff, "Studies on the effect of pH on the sorption of  $\text{Pb}^{2+}$   $\text{Cd}^{2+}$  from aqueous solutions by bicolor Cocoyam) biomass," *Electronic Journal of Biotechnology*, vol. 7, no. 3, pp. 313–323, 2004.
- [37] H. Tamura, A. Tanaka, K.-Y. Mita, and R. Furuichi, "Surface hydroxyl site densities on metal oxides as a measure for the ion-exchange capacity," *Journal of Colloid and Interface Science*, vol. 209, no. 1, pp. 225–231, 1999.
- [38] K. Y. Foo and B. H. Hameed, "Insights into the modeling of adsorption isotherm systems," *Chemical Engineering Journal*, vol. 156, pp. 2–10, 2010.
- [39] P. J. P. Chen, *Decontamination of Heavy Metals: Processes, Mechanisms, and Applications*, Taylor & Francis, Abingdon, UK, 2012.
- [40] R. Elmoubarki, F. Z. Mahjoubi, H. Tounsadi et al., "Adsorption of textile dyes on raw and decanted Moroccan clays: Kinetics, equilibrium and thermodynamics," *Water Resources and Industry*, vol. 9, pp. 16–29, 2015.
- [41] O. S. Bello, M. A. Oladipo, and A. M. Olatunde, "Sorption studies of lead ions onto activated carbon produced from Oil-Palm fruit fibre," *Stem Cell*, vol. 1, no. 1, pp. 14–29, 2010.
- [42] H. Shahbeig, N. Bagheri, S. A. Ghorbanian, A. Hallajisani, and S. Poorkarimi, "A new adsorption isotherm model of aqueous solutions on granular activated carbon," *World Journal of Modelling and Simulation*, vol. 9, no. 4, pp. 243–254, 2013.
- [43] M. B. Desta, "Batch sorption experiments: Langmuir and Freundlich isotherm studies for the adsorption of textile metal ions onto Teff straw (*Eragrostis tef*) agricultural waste," *Journal of Thermodynamics*, vol. 2013, Article ID 375830, 6 pages, 2013.
- [44] Y. Bulut and Z. Tez, "Removal of heavy metals from aqueous solution by sawdust adsorption," *Journal of Environmental Sciences*, vol. 19, no. 2, pp. 160–166, 2007.

- [45] A. U. Itodo and H. U. Itodo, "Sorption energies estimation using Dubinin-Radushkevich and Temkin adsorption isotherms," *Life Science Journal*, vol. 7, no. 4, pp. 31-39, 2010.
- [46] M. A. Al-Anber, "Thermodynamics approach in the adsorption of heavy metals," in *Thermodynamics—Interaction studies—Solids, Liquids and Gases*, J. C. Moreno-Pirajan, Ed., pp. 737-764, InTech, Rijeka, Croatia, 2011.
- [47] A. O. Dada, A. P. Olalekan, A. M. Olatunya, and O. Dada, "Langmuir, Freundlich, Temkin and Dubinin-Radushkevich isotherms studies of equilibrium sorption of  $Zn^{2+}$  unto phosphoric acid modified rice husk," *IOSR Journal of Applied Chemistry*, vol. 3, no. 1, pp. 38-45, 2012.
- [48] Z. Ren, G. Zhang, and J. Paul Chen, "Adsorptive removal of arsenic from water by an iron-zirconium binary oxide adsorbent," *Journal of Colloid and Interface Science*, vol. 358, no. 1, pp. 230-237, 2011.
- [49] M. H. Ehrampoush, M. Miria, M. H. Salmani, and A. H. Mahvi, "Cadmium removal from aqueous solution by green synthesis iron oxide nanoparticles with tangerine peel extract," *Journal of Environmental Health Science and Engineering*, vol. 13, no. 1, article 84, 2015.
- [50] T. V. J. Charpentier, A. Neville, J. L. Lanigan, R. Barker, M. J. Smith, and T. Richardson, "Preparation of magnetic carboxymethylchitosan nanoparticles for adsorption of heavy metal ions," *ACS Omega*, vol. 1, pp. 77-83, 2016.
- [51] J. Gong, L. Chen, G. Zeng et al., "Shellac-coated iron oxide nanoparticles for removal of cadmium(II) ions from aqueous solution," *Journal of Environmental Sciences (China)*, vol. 24, no. 7, pp. 1165-1173, 2012.



**Hindawi**

Submit your manuscripts at  
<https://www.hindawi.com>

